Nanostructured Graphene Composite Papers for Highly Flexible and Foldable Supercapacitors

Lili Liu, Zhiqiang Niu, Li Zhang, Weiya Zhou, Xiaodong Chen, and Sishen Xie*

Recent development in portable electronics has promoted the increasing demand for high-performance energy-storage systems that are lightweight, ultrathin, flexible, wearable, and even foldable.[1–6] Among various energy-storage systems, supercapacitors are an important class of energy-storage devices that have attracted significant attention because of their higher power density, cycle efficiency, and charge/discharge rates as against batteries.[7–10] However, conventional supercapacitors are still too heavy, thick, rigid, and bulky to meet the practical requirements for portable devices due to the employment of inactive components, including current collector, binder, and conductive additives.[11,12] As such, there is an urgent need to develop flexible or even foldable supercapacitors, which are strongly dependent on the innovation of electrode materials and the design of suitable configuration.[13]

Flexible supercapacitors require their electrode materials to possess good electrical and mechanical properties, high power/energy densities, excellent cyclic stability, and the capacity to accommodate large levels of strain without sacrificing performance.[13–32] Recently, integration of functional materials including carbon nanotubes, metal oxides as well as conductive polymers, into various flexible substrates, such as plastics, textiles, and papers, was achieved to fabricate flexible supercapacitor electrodes.[33–40] Among these substrates, paper that is composed of cellulose fibers (CFs) exhibits a set of properties that is different from that of flat plastics used as conventional flexible substrates due to the natural features of CFs and their porous structure.[41] For example, the large number of surface functional groups on the CF surface is beneficial for binding additional functional materials, and its rough and porous structure is preferred from the viewpoint of fast mass and electron transport kinetics. Furthermore, CF paper is also recyclable, environmentally friendly, low-cost, and easily processable.[42–46] Therefore, CF paper could be a good substrate on which to fabricate lightweight and flexible composite paper electrodes for supercapacitors by the incorporation of functional materials.

As a fundamental two-dimensional (2D) carbon structure, graphene and its derivatives have been incorporated into CF paper as the electrode material of supercapacitors due to their large surface area, high conductivity, and good mechanical strength.[47–50] Currently, graphene/CF composite paper electrodes are generally fabricated by filtering graphene-coated CFs into composite paper or directly assembling graphene sheets into the pores of the paper.[47–49] However, these two methods cannot make full use of the CF network and the porous structure of paper. For example, for graphene/CF composite paper fabricated by filtering graphene-coated CF solution, the graphene sheets are usually attached on the surface of CFs and the inner pores of paper are not effectively utilized.[47] While in graphene/CF composite paper obtained by filtering graphene suspension through filter paper, the graphene sheets are directly deposited in the pores of CF paper; as a result, they are randomly oriented and seriously aggregated.[49]

Coating the CFs with a thin electric phase to form composite paper is considered an ideal approach to form an electric network with high electron-transport ability due to the network structure of CF paper.[47] Moreover, the inner pores of paper can provide space for loading and assembling active electrode materials into microscale porous architectures, which can display the functional properties of active electrode materials. If we could fully utilize the CF network and the porous structure in paper by controllably assembling graphene onto the CF network and into the pores of paper, nanostructured graphene architecture would be formed in the composite paper, which would lead to enhanced performance in energy storage, environmental remediation, and so on.

Here, we employ a "dipping and drying" strategy to coat a thin and uniform graphene oxide (GO) layer onto the surface of the CFs in the paper and then use a hydrothermal process to assemble GO sheets into microscale porous reduced graphene oxide (rGO) networks in the pores of paper, to form rGO/CF composite paper with a nanostructured rGO architecture. Such nanostructured rGO composite paper fully utilizes the CF network and the porous structure in paper; it not only ensures that the electrons are readily transported throughout the CF network, but also overcomes the aggregation of rGO sheets in the pores of paper and facilitates the penetration of liquid ions. These advantages make nanostructured rGO/CF composite paper a promising substrate on which to deposit other functional materials to further improve its electrochemical properties by combining the diverse functionalities and synergistic effect of graphene and functional materials. As a proof of concept, polyaniline (PANI) is deposited onto the rGO surface in rGO/CF composite paper, forming PANI-rGO/CF composite paper. Furthermore, we demonstrate that the resultant

Dr. L. Liu,[+] Dr. Z. Niu,[+] Dr. L. Zhang, Prof. X. Chen
School of Materials Science and Engineering
Nanyang Technological University
50 Nanyang Avenue, Singapore 639798
E-mail: chenxd@ntu.edu.sg
Prof. W. Zhou, Prof. S. Xie
Beijing National Laboratory for Condensed Matter Physics
Institute of Physics, Chinese Academy of Sciences
Beijing 100190, China
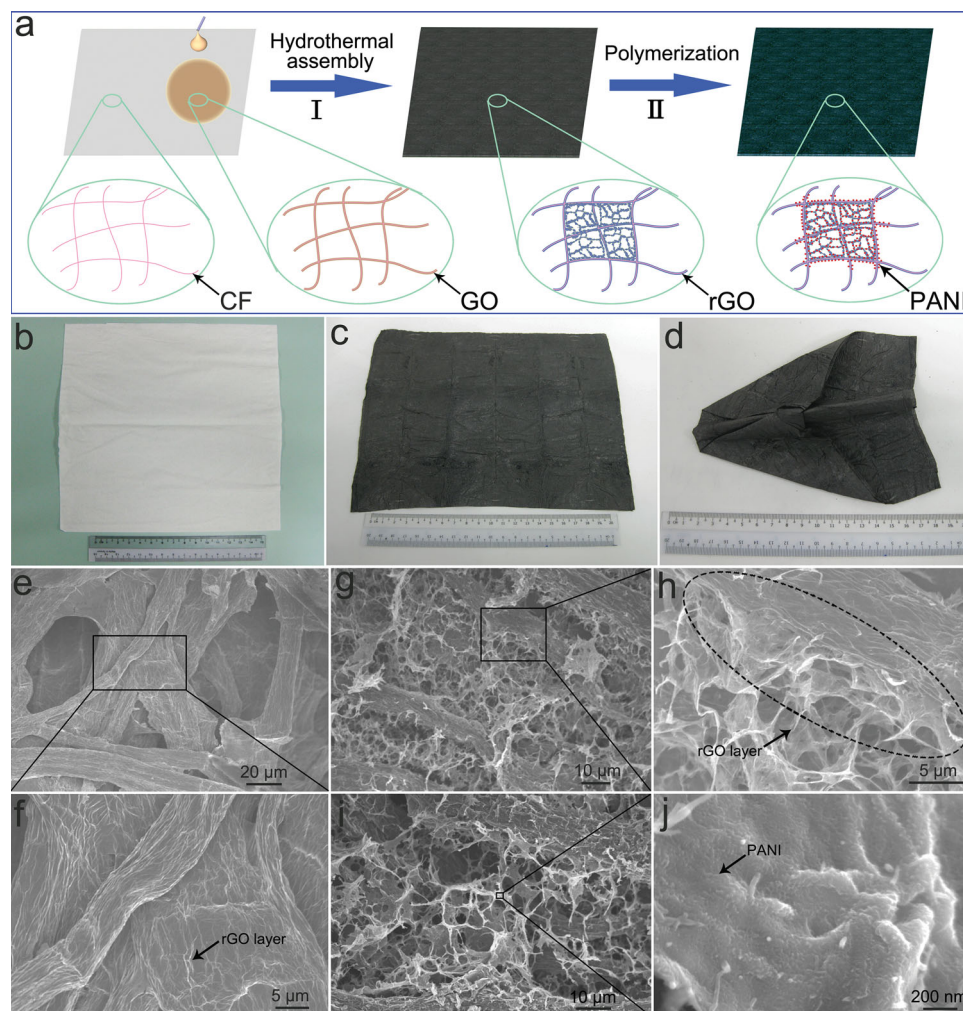[+]These authors contributed equally to this work

Figure 1. a) Schematic diagram of preparing PANI-rGO/CF composite paper. Optical images of b) pure CF paper and c,d) nanostructured rGO/CF composite paper. SEM images of e,f) rGO-coated CF paper, g,h) nanostructured rGO/CF composite paper, and i,j) PANI-rGO/CF composite paper.

PANI-rGO/CF composite papers show potential applications to serve as flexible electrodes for supercapacitors with different configurations.

Figure 1a schematically shows the experimental preparation of PANI-rGO/CF composite paper. In a typical experiment, the GO aqueous suspension was first dropped onto the surface of CF paper (Figure 1b) until the GO dispersion was saturated, taking care that the surface of paper was kept flat to make the GO suspension uniform distribution in the paper. After drying, the GO sheets were coated tightly onto the surface of CFs due to covalent bonding through the amine–epoxide reaction between functional epoxy groups on GO sheets and amine in the CFs, which formed GO-coated CF paper.[51] Subsequently, the GO-coated CF paper was directly used as a template to assemble GO sheets into microscale porous rGO networks in the pores of the paper by a hydrothermal process (step I of Figure 1a), to form nanostructured rGO/CF composite paper (Figure 1c). Followed by freeze-drying of rGO/CF paper, a chemical polymerization process was used to deposit PANI on the rGO surface in rGO/CF paper to obtain PANI-rGO/CF composite paper, as shown in step II of Figure 1a. The "dipping and drying" process is

similar to layer-by-layer assembly,[52] which is known as a highly versatile method for fabrication of controlled layered structures. Therefore, we expect that our system may also have controlled structures.

To characterize the morphology of GO layers on the surface of CFs by scanning electron microscopy (SEM), the GO-coated CF paper was chemically reduced by hydrazine mono-hydrate, to form conductive rGO-coated CF paper, as the GO sheets are typically insulating, which can be ascribed to the sp³ C–O bonding.[53–57] SEM images (Figure 1e,f) clearly indicate that rGO sheets are only coated on the surface of CFs in paper tightly and almost no rGO sheet aggregated in the pores of paper, which left the porous structure of the original CF paper. Furthermore, several wrinkles were formed on the surface of rGO layers. A richly wrinkled structure could improve the active area of rGO layers.[58] Raman spectra also suggest that the GO layers coated on the surface of CFs was chemically converted into rGO layers after the chemical reduction, as shown in **Figure 2**a.[59,60]

The sheet resistance of rGO-coated CF paper reaches about 1.1 kΩ sq^{-1} since the rGO layer coating on the CF surface is
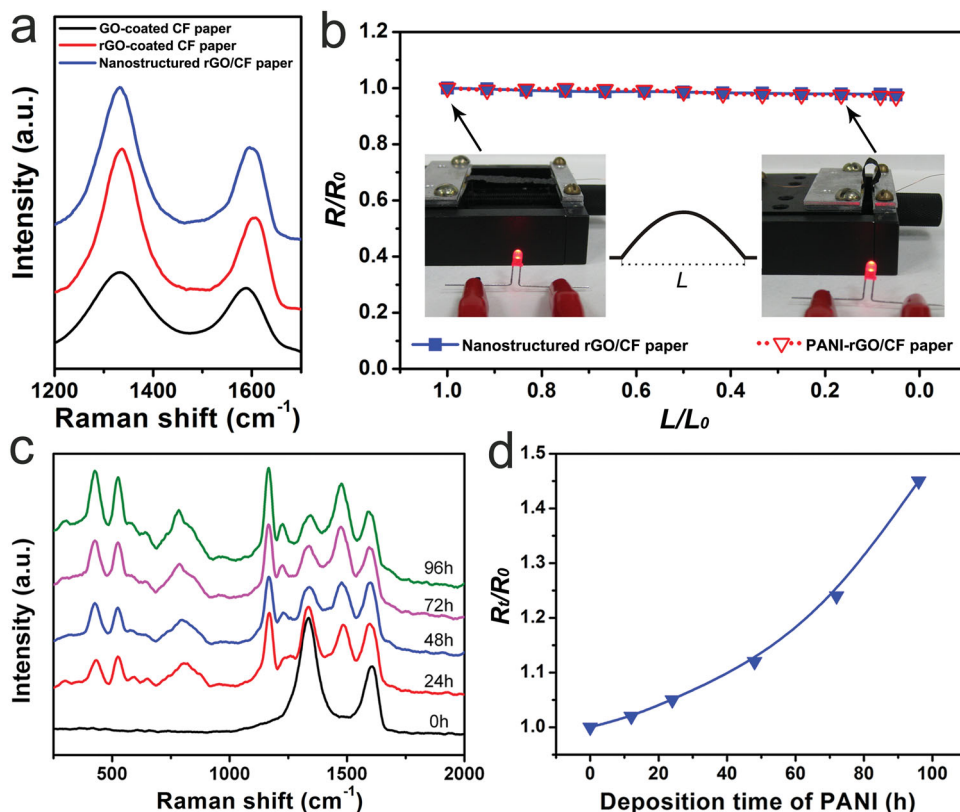
Figure 2. a) Raman spectra of GO-coated CF paper, rGO-coated CF paper, and nanostructured rGO/CF paper. b) The normalized sheet resistance of nanostructured rGO/CF and PANI-rGO/CF composite papers in different bending states, where R_0 is the initial resistance of composite papers and R is the resistance of composite papers in different bending states, L_0 is the initial length of papers, and L is the distance between two ends of papers in different bending states (middle inset). Insets: optical images of an LED illuminated by using nanostructured rGO/CF composite paper as the connecting wire in different bending states. c) Raman spectra of PANI-rGO/CF composite papers with different PANI deposition time at $\lambda = 633$ nm. d) The sheet resistance of PANI-rGO/CF composite papers with different PANI deposition time, where R_0 is the resistance of nanostructured rGO/CF composite paper and R_t is the resistance of PANI-rGO/CF papers with different PANI deposition times.

helpful for electron transport through the composite paper. Although the sheet resistance of rGO-coated CF paper could be further reduced by more "dipping–drying", some pores of the paper were filled and covered by compact rGO layers (Supporting Information, Figure S1), which formed compact rGO/CF paper. As a result, the accessible surface area of rGO sheets in paper was lost, and their practical applications as energy-storage electrodes were limited. To prevent the aggregation of rGO sheets in the pores of rGO-coated CF paper, the GO sheets were assembled into microscale porous rGO networks in the pores of paper by a hydrothermal process instead of repeatedly "dipping–drying" (step I of Figure 1a), to form nanostructured rGO/CF composite paper. Furthermore, during the hydrothermal process, the GO layers on the surface of CFs were also reduced into rGO layers and no additional reduction process was required. Raman (Figure 2a) and Fourier-transform infrared (FTIR, Figure S2) spectra suggest that the chemical conversion from GO to rGO occurred and that rGO structures formed in the CF paper.[60] The rGO networks in the pores of rGO-coated paper possess a continuously cross-linked structure with pore sizes in the range of sub-micrometer to several micrometers (Figure 1g). In addition, microscale rGO networks connect well with the neighboring rGO layers on the surface

of CFs, as illustrated in the dashed ellipse of Figure 1h. Such connections would have an advantage in transporting electrons from microscale rGO networks in the pores to the rGO-coated CF network, and would lead to low sheet resistance (about 0.21 kΩ sq^{-1}). As a control experiment, we directly fabricated rGO networks in the pores of pure CF papers by the same hydrothermal process. The sheet resistance of the resulting papers (0.65 kΩ sq^{-1}) is much larger than that of nanostructured rGO/CF composite paper fabricated by combining "dipping–drying" with the hydrothermal process, indicating that a hierarchical rGO architecture with good connections in nanostructured rGO/CF composite paper effectively enhances the electron transport.

The presence of a nanostructured rGO architecture in rGO/CF composite paper almost has no effect on the flexibility of the paper (Figure 1d). Furthermore, the tensile strength and Young's modulus of the nanostructured rGO/CF paper are about 1.2 and 20.5 MPa (Figure S3), respectively. These values are larger than those of CF paper (tensile strength: 0.73 MPa, Young's modulus: 18.3 MPa). As a result, the nanostructured rGO/CF composite paper can be rolled up, bent, or twisted easily, and even folded without any cracking. Furthermore, during these processes, rGO is not removed, which indicates

**ADVANCED
MATERIALS**

www.advmat.de

*Materials
Views*

www.MaterialsViews.com

the excellent adhesion between rGO sheets and CFs in the composite paper. More importantly, the sheet resistance of the nanostructured rGO/CF composite paper is nearly unchanged even at a very high level of bending (Figure 2b), which suggests that the conductance of the nanostructured rGO/CF composite paper is nearly unaffected by the bending stress. Furthermore, the conductance of the nanostructured rGO/CF composite paper remained nearly constant after 100 bending cycles (Figure S4), which indicates the mechanical stability and durability of nanostructured rGO/CF composite paper. To demonstrate the flexibility of nanostructured rGO/CF composite paper via simple visual cues, we use nanostructured rGO/CF composite paper as the connecting wire to illuminate a light-emitting diode (LED) (inset of Figure 2b). The nanostructured rGO/CF composite paper worked well in a high bending state (inset of Figure 2b).

The nanostructured rGO/CF composite paper possesses a porous hierarchical rGO architecture with high electron-transport ability and good mechanical properties, which makes it an ideal substrate on which to deposit other functional materials for various applications. PANI is considered to be one of the most promising pseudocapacitance electrode materials because of its relatively higher conductivity and lower cost than many other conducting polymers.[61–67] Therefore, PANI was formed in the rGO surface in the nanostructured rGO/CF composite paper to improve its performance by chemical oxidation polymerization (step II of Figure 1a). During the process of depositing PANI, the porous rGO architecture in rGO/CF paper enables aniline molecules to infiltrate into the inner of rGO/CF paper easily and efficiently. In addition, rGO/CF paper maintains its integrity during the deposition process due to its good mechanical strength as well as toughness. After performing the polymerization, small PANI nanoparticles formed on the rGO surface in the rGO/CF paper, which yielded PANI-rGO/CF composite paper, as shown in Figure 1i,j. The resultant PANI-rGO/CF composite paper still possesses a porous structure (Figure 1i). Raman spectra (Figure 2c) and FTIR (Figure S3) spectra also prove the formation of PANI in the composite paper.[64] Furthermore, the intensity of peaks corresponding to PANI is increased with the increase of PANI deposition time, as shown in Figure 2c, which indicates that more and more PANI was deposited on the surface of rGO in the PANI-rGO/CF composite paper.[64] The tensile strength and Young's modulus of the PANI-rGO/CF paper reach about 1.9 and 27.2 MPa, respectively, and the PANI-rGO/CF composite paper still retains the high flexibility of paper. Therefore, there is nearly no significant degradation of its sheet resistance in different bending states, as with nanostructured rGO/CF paper, as shown in Figure 2b.

Since our resultant PANI-rGO/CF composite paper is free-standing and conductive, it can be used as supercapacitor electrodes in which neither an insulating binder nor a low capacitance conducting additive is required. These electrodes are quite different from the conventional rGO/PANI powder electrodes, as depicted in Figure S5. In conventional rGO/PANI powder electrodes, the electrons have to be transported through binder or PANI–PANI contact between rGO/PANI sheets, which leads to high resistance (Figure S5a).[64] In contrast, in our case, the electrons are readily transported throughout the PANI-rGO network with low resistance (Figure S5b). The performance

of PANI-rGO/CF composite paper was first tested in a conventional supercapacitor configuration (Figure S6). Two redox peaks are observed in the CV curve of the conventional supercapacitors based on PANI-rGO/CF composite paper (**Figure 3**a) due to the faradic reaction from PANI, corresponding to its leucoemeraldine/emeraldine and emeraldine/pernigraniline structural conversions, respectively.[65] The curve is different from the rectangular shape of the supercapacitors based on nanostructured rGO/CF paper (Figure 3a), which indicates a good electrical-double-layer performance.[12,21,60] This difference is also testified by their charge/discharge curves, as shown in Figure 3b. The specific capacitance of PANI-rGO/CF paper with a PANI deposition time of 72 h can reach up to 464 F g^{-1} based on PANI and rGO mass only, which is much larger than the case of nanostructured rGO/CF composite paper (212 F g^{-1}), as shown in Figure 3d. This result suggests that the specific capacitance of PANI-rGO/CF paper is remarkably improved due to its additional pseudocapacitance, which originates from PANI. However, further increasing of the PANI deposition time would lead to the decrease of specific capacitance for PANI-rGO/CF composite paper, which may be because some pores in the composite paper are filled by PANI (Figure S7) and the conductivity of the composite paper is decreased (Figure 2d) due to the deposition of more PANI. In addition, the specific capacitance of nanostructured rGO/CF composite paper (212 F g^{-1}) is much higher than that of compact rGO/CF paper (72 F g^{-1}), as shown in Figure 3a,b. Furthermore, the specific capacitance of nanostructured rGO/CF composite paper drops less abruptly with the increase of the scan rate in comparison with that of compact rGO/CF paper (Figure 3c). These observations indicate that the porous rGO architecture effectively overcomes the aggregation of rGO sheets in pores of nanostructured rGO/CF paper and facilitates the diffusion of ions from the electrolyte to the inner regions of nanostructured rGO/CF paper, as depicted in Figure 3e,f.[58]

As energy-storage devices, some practical applications of supercapacitors require the supercapacitors not only to provide high performance, but also to be small and lightweight. To meet these demands, a compact supercapacitor configuration which is different from the conventional configuration should be considered. Since PANI-rGO/CF composite papers possess high flexibility and low sheet resistance, they can be directly used as electrodes for supercapacitors where flexible electrodes are required. As a proof of concept, we fabricated all-paper compact supercapacitors based on PANI-rGO/CF composite paper, as depicted in **Figure 4**a. This format is different from the conventional supercapacitor, in which extra metallic foils or foams are generally used as current collectors owing to the poor conductivity of active electrode materials. The use of metallic current collectors makes the supercapacitors too heavy or bulky, restricting the use of these supercapacitors in the applications that are constrained by space and weight.[1] In contrast, in our case, use of PANI-rGO/CF paper with low resistance makes it possible for Pt wire to replace extra bulky metallic foils or foams as current collectors. Pt wire has a small diameter and can be bent or twisted, and even folded easily; as a result, it has almost no effect on the compact structure of supercapacitors. The calculated specific capacitance of PANI-rGO/CF paper in the compact supercapacitor is about 292 F g^{-1} (Figure S8). Compact
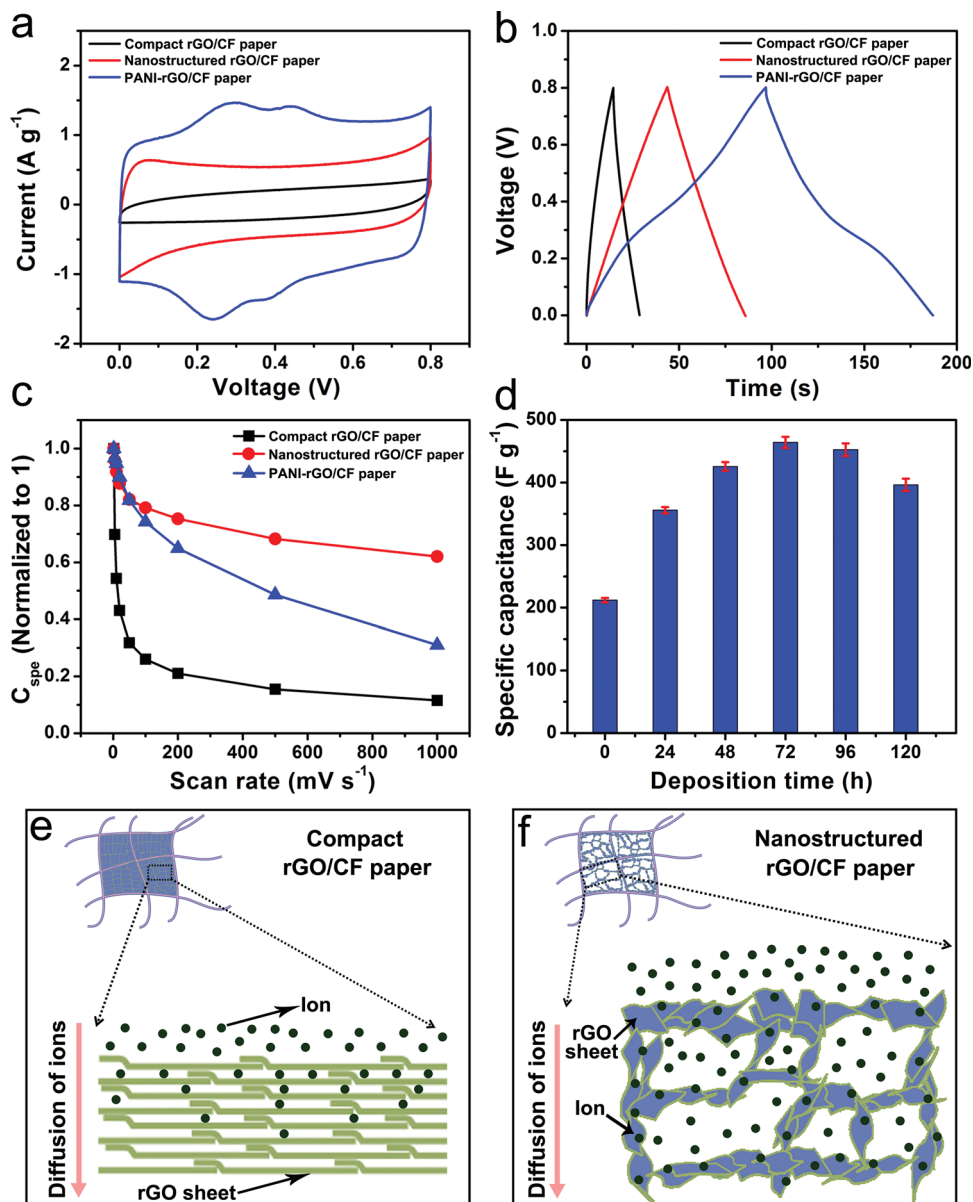
Materials
Views
www.MaterialsViews.com

ADVANCED
MATERIALS
www.advmat.de

COMMUNICATION

Figure 3. a) CV curves with a scan rate of 10 mV s^{-1} and b) charge/discharge curves at a current of 1 A g^{-1} of conventional supercapacitors based on compact rGO/CF composite paper, nanostructured rGO/CF composite paper, and PANI-rGO/CF composite paper (PANI deposition time: 72 h). c) Comparison of the normalized specific capacitance between compact rGO/CF composite paper, nanostructured rGO/CF composite paper, and PANI-rGO/CF paper (PANI deposition time: 72 h) at different scan rates. d) Specific capacitance of the PANI-rGO/CF papers with different PANI deposition time. Schematic diagrams of ion diffusion in e) compact rGO/CF composite paper and f) nanostructured rGO/CF composite paper.

design of PANI-rGO/CF paper supercapacitors brings in new opportunities for advanced applications in energy-storage devices with high performance and lightweight architecture.

All-solid-state integrated supercapacitors are favored over their liquid counterparts for the consideration of encapsulation and safety since they possess high physical flexibility, desirable electrochemical properties, and excellent mechanical integrity.[68,69] Therefore, we fabricated all-solid-state integrated supercapacitors based on PANI-rGO/CF composite paper, as depicted in Figure 4c. To demonstrate their flexibility and foldability, we measured the CV curves of a representative supercapacitor before and after both bending and folding, as shown

in Figure 4d. There was only a very slight difference in the CV curves when the all-solid-state supercapacitor based on PANI-rGO/CF composite paper was rolled up and folded. The calculated specific capacitance of PANI-rGO/CF composite paper in all-solid-state supercapacitor is about 224 F g^{-1} (Figure S9a), and the paper maintained 89 % of the maximum capacity after 1000 cycles (Figure S9b), which indicates a good recycling stability. In addition, the variations in specific capacitance of the all-solid-state supercapacitor based on PANI-rGO/CF composite paper in different bending and folding states are shown in Figure 4e,f. The specific capacitance of the resultant all-solid-state supercapacitor lost about 3.4 % and 5 % of maximum capacity,
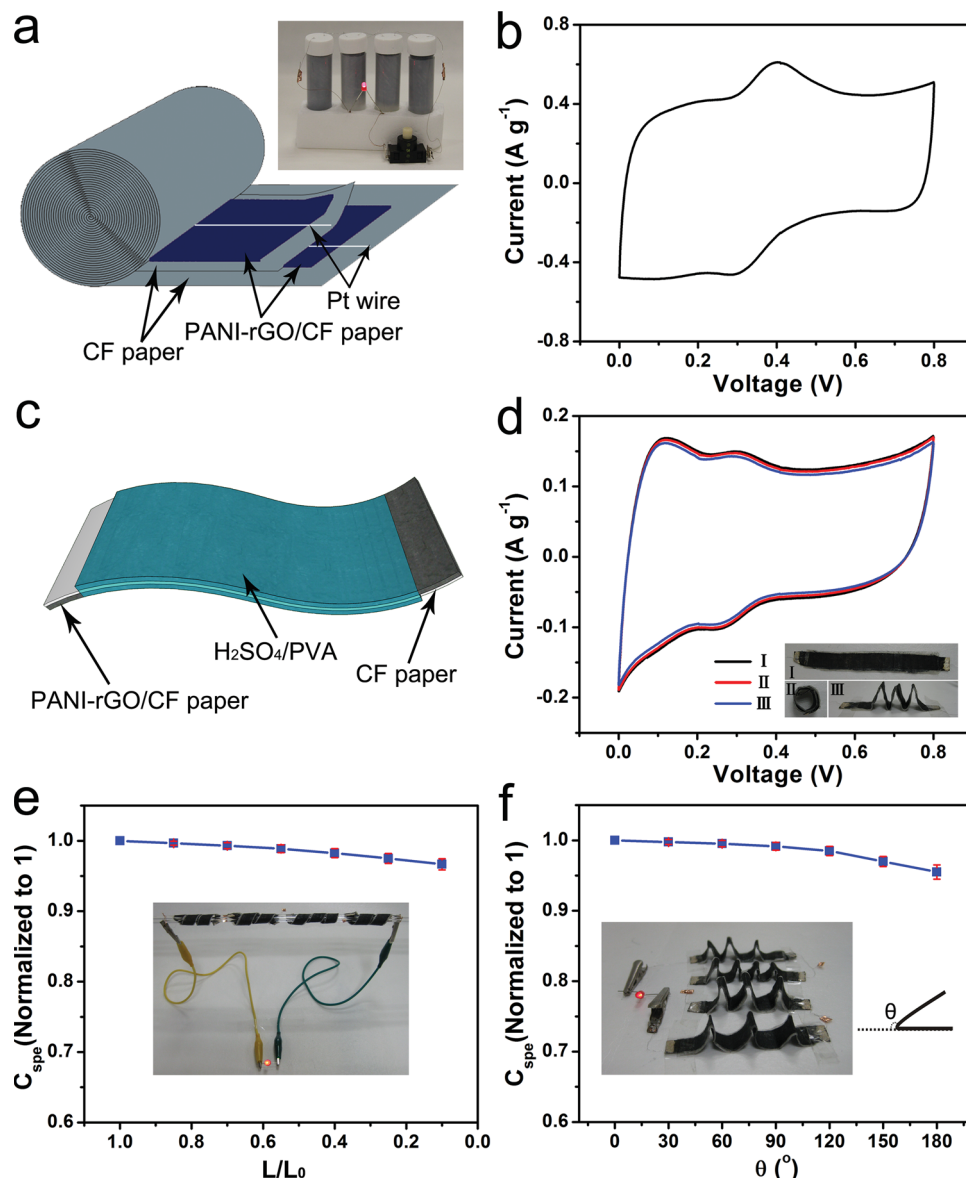
Figure 4. a) Schematic diagram of a compact supercapacitor based on PANI-rGO/CF paper. Inset: optical image of four compact supercapacitors used to light an LED. b) CV curve of the compact supercapacitor, scan rate: 5 mV s^{-1}. c) Schematic diagram of an all-solid-state integrated supercapacitor based on PANI-rGO/CF paper. d) CV curves of the all-solid-state supercapacitor under different states, scan rate: 2 mV s^{-1}. Variations of specific capacitances of the all-solid-state supercapacitor in different e) bending and f) folding states. The specific capacitance in the original state is normalized to 1. Insets: optical images of an LED illuminated by using four all-solid-state integrated supercapacitors in twisting and folding states, respectively.

respectively, when the supercapacitor was bent to 10 % of its original length ($L/L_0 = 0.1$) and folded by 180° ($\theta = 180°$). These results suggest that the all-solid-state supercapacitor based on PANI-rGO/CF composite paper is stable when bent and folded. To demonstrate the flexibility and foldability of the resultant all-solid-state supercapacitors via simple visual cues, we prepared four supercapacitor units in series to light a red LED. The all-solid-state supercapacitors could light the LED when they were twisted and folded, even throughout the bending and folding process, as shown in the inset of Figure 4e,f and video S1.

In summary, nanostructured rGO/CF composite paper was fabricated by combining "dipping and drying" with a hydrothermal process. rGO sheets were uniformly coated on

the surface of the CF network and assembled into microscale porous networks in the pores of the paper. Both the CF network and porous structure of paper are fully utilized. Furthermore, the rGO layers on the surface of the CF network are well connected with the microscale rGO networks in the pores of the paper, which results in low sheet resistance. More importantly, the nanostructured rGO/CF composite paper maintains the high flexibility and good mechanical properties of CF paper and its sheet resistance is nearly unchanged even in a very high bending state. Therefore, our paper could broaden applications of nanostructured rGO/CF composite paper in flexible electronics, energy-storage electrodes, antistatic packages, electromaganetic shielding, and sensors. In addition, nanostructured

rGO/CF composite paper could be used as a substrate for further incorporation of other functional materials to diversify the performance of rGO/CF composite paper. As a proof of concept, the PANI with pseudocapacitive properties was deposited on the rGO surface in the nanostructured rGO/CF paper to form PANI-rGO/CF composite paper. A high specific capacitance of 464 F g^{-1} is achieved for PANI-rGO/CF composite paper. Based on the PANI-rGO/CF composite paper, two kinds of supercapacitors with compact design and all-solid-state configuration were fabricated. Compact design endows the supercapacitors with a simplified and lightweight architecture, which brings in new opportunities for advanced applications in energy-storage devices that are constrained by space and weight. The high flexibility, foldability, and performance stability of all-solid-state integrated supercapacitors will pave the way for advanced applications in the area of energy-storage devices to be compatible with flexible, wearable and/or printable electronics.

Experimental Section

Fabrication of rGO-Coated CF Paper: An aqueous GO dispersion was first prepared by oxidizing graphite powder by using a modified Hummers method.[70] The aqueous GO dispersion (2.0 mg mL^{-1}) was dropped onto the surface of the CF paper (three-ply tissues) until the paper was saturated, taking care that the surface of paper should be kept flat. After drying, the GO-coated CF paper was obtained. To chemically reduce the GO sheets on the surface of CFs in the paper, the GO-coated CF paper was placed in an autoclave, and 100 μL hydrazine monohydrate (98 %) was added to the autoclave. After that, the autoclave was heated at 90 °C for 6 h.

Fabrication of Nanostructured rGO/CF Composite Paper: The GO-coated CF paper was rolled up and placed in an autoclave. Then, the aqueous GO dispersion (3.5 mg mL^{-1}), hydrazine monohydrate, and ammonia solution with a volume ratio of 286:1.1:1 were added to the autoclave just over the GO-coated CF paper. After that, the autoclave was heated at 90 °C for 2 h. The resultant rGO/CF paper was washed in deionized water to purge hydrazine monohydrate. After freeze-drying, nanostructured rGO/CF paper was obtained.

Fabrication of Compact rGO/CF Composite Paper: The aqueous GO dispersion (2.0 mg mL^{-1}) was dropped onto the surface of the CF paper and then the GO-coated CF paper was dried at room temperature. After repeating this "dipping and drying" process three times, the GO-coated CF paper and 100 μL hydrazine monohydrate (98 %) were placed in an autoclave, which was then heated to 90 °C for 6 h. After heat treatment, the compact rGO/CF paper was obtained.

Fabrication of PANI-rGO/CF Composite Papers: Aniline monomers were polymerized on the nanostructured rGO/CF paper by a chemical method. The nanostructured rGO/CF paper was immersed in 0.2 M aniline solution (solvent 1 M HCl) in a vacuum vessel for several minutes. An equal volume of precooled 0.2 M ammonium persulfate (APS) solution was added to the aniline solution dropwise. After that, the mixture was kept at 0°C–5 °C for different time periods. The as-prepared PANI-rGO/CF composite paper was washed with deionized water. Finally, PANI-rGO/CF composite paper was obtained by freeze-drying.

Fabrication of Conventional Supercapacitors: The conventional supercapacitors based on compact rGO/CF composite paper, nanostructured rGO/CF composite paper, and PANI-rGO/CF composite paper were prepared as depicted in Figure S6. Pt slices were used as current collectors. CF paper served as a separator and the electrolyte was H$_2$SO$_4$ (1 M). The electrode materials and separator were stacked and electrolyte was sandwiched between them, as shown in Figure S6.

Fabrication of Compact Supercapacitors Based on PANI-rGO/CF Composite Paper: The PANI-rGO/CF paper and the pure CF paper were first cut to a certain size to match the demand of the designed supercapacitor

electrodes, respectively. Then, the PANI-rGO/CF composite paper and pure CF paper were stacked together, and two Pt wires with the diameter of 100 μm were sandwiched between the PANI-rGO/CF composite paper and pure CF paper, as depicted in Figure 4a. After rolling up, the papers were assembled into a suitable container and 1 M H$_2$SO$_4$ was filled.

All-Solid-State Integrated Supercapacitors Based on PANI-rGO/CF Composite Paper: Firstly, the H$_2$SO$_4$-polyvinylacetate (PVA) gel electrolyte was prepared as follows: 3 g H$_2$SO$_4$ were mixed with 30 mL deionized water and then 3 g PVA powder were added. The whole mixture was heated up to 85 °C under vigorous stirring until the solution became clear. Then, the solution was kept at 85 °C without stirring. Secondly, PANI-rGO/CF composite paper and the pure CF paper with desired size were stacked together on a glass slide and two Pt wires with the diameter of 100 μm were sandwiched between the PANI-rGO/CF paper and pure CF paper, as depicted in Figure 4c. Subsequently, a H$_2$SO$_4$/PVA solution was dropped on their surface, while care was taken to ensure that one end of PANI-rGO/CF paper was not contacted with H$_2$SO$_4$/PVA solution to function as the electrical contact of the electrode with the conductive wire. Subsequently, the sample was left in the fume hood at room temperature for several hours to vaporize the excess water, which formed the all-solid-state integrated supercapacitor. After that, the as-prepared all-solid-state integrated supercapacitor was peeled off the glass.

Characterization: The morphology and the microstructures of composite paper were characterized by using FE-SEM (JSM-7600F). The sheet resistance of the composite paper was measured by using a 4200-SCS Semiconductor Characterization System. The mechanical properties of the composite paper were tested on a tensile-testing machine (DMA Q800). Cyclic voltammetry of the supercapacitors was performed by using a CHI 660D instrument (CHI Instruments). The galvanostatic charge/discharge of the supercapacitors at an operation voltage range of 0–0.8 V was carried out on a supercapacitor test system (Solartron, 1470E).

Supporting Information

Supporting Information is available from the Wiley Online Library or from the author.

Acknowledgements

[1] G. Zhou, F. Li, H. M. Cheng, *Energy Environ. Sci.* **2014**, 7, 1307.
[2] Y. G. Wang, Y. Y. Xia, *Adv. Mater.* **2013**, 25, 5336.
[3] Z. Song, T. Ma, R. Tang, Q. Cheng, X. Wang, D. Krishnaraju, R. Panat, C. K. Chan, H. Yu, H. Jiang, *Nat. Commun.* **2014**, 5, 3140.
[4] X. W. Yang, C. Cheng, Y. F. Wang, L. Qiu, D. Li, *Science* **2013**, 341, 534.
[5] V. L. Pushparaj, M. M. Shaijumon, A. Kumar, S. Murugesan, L. Ci, R. Vajtai, R. J. Linhardt, O. Nalamasu, P. M. Ajayan, *Proc. Natl. Acad. Sci. USA* **2007**, 104, 13574.
[6] K. Xie, B. Wei, *Adv. Mater.* **2014**, DOI: 10.1002/adma.201305919.

COMMUNICATION

[7] Y. Huang, J. Liang, Y. Chen, *Small* **2012**, *8*, 1805.

[8] Y. Sun, Q. Wu, G. Shi, *Energy Environ. Sci.* **2011**, *4*, 1113.

[9] P. Simon, Y. Gogotsi, *Nat. Mater.* **2008**, *7*, 845.

[10] X. Yu, B. Lu, Z. Xu, *Adv. Mater.* **2014**, *26*, 1044.

[11] Y. M. He, W. J. Chen, C. T. Gao, J. Y. Zhou, X. D. Li, E. Q. Xie, *Nanoscale* **2013**, *5*, 8799.

[12] Z. Q. Niu, W. Y. Zhou, J. Chen, G. X. Feng, H. Li, W. J. Ma, J. Z. Li, H. B. Dong, Y. Ren, D. Zhao, S. S. Xie, *Energy Environ. Sci.* **2011**, *4*, 1440.

[13] Z. Q. Niu, H. B. Dong, B. W. Zhu, J. Z. Li, H. H. Hng, W. Y. Zhou, X. D. Chen, S. S. Xie, *Adv. Mater.* **2013**, *25*, 1058.

[14] L. Nyholm, G. Nystrom, A. Mihranyan, M. Stromme, *Adv. Mater.* **2011**, *23*, 3751.

[15] N. S. Liu, W. Z. Ma, J. Y. Tao, X. H. Zhang, J. Su, L. Y. Li, C. X. Yang, Y. H. Gao, D. Golberg, Y. Bando, *Adv. Mater.* **2013**, *25*, 4925.

[16] J. Ren, W. Y. Bai, G. Z. Guan, Y. Zhang, H. S. Peng, *Adv. Mater.* **2013**, *25*, 5965.

[17] C. J. Yu, C. Masarapu, J. P. Rong, B. Q. Wei, H. Q. Jiang, *Adv. Mater.* **2009**, *21*, 4793.

[18] Y. W. Cheng, S. T. Lu, H. B. Zhang, C. V. Varanasi, J. Liu, *Nano Lett.* **2012**, *12*, 4206.

[19] M. Kaempgen, C. K. Chan, J. Ma, Y. Cui, G. Gruner, *Nano Lett.* **2009**, *9*, 1872.

[20] G. H. Yu, L. B. Hu, N. A. Liu, H. L. Wang, M. Vosgueritchian, Y. Yang, Y. Cui, Z. A. Bao, *Nano Lett.* **2011**, *11*, 4438.

[21] Z. Q. Niu, L. L. Liu, L. Zhang, Q. Shao, W. Y. Zhou, X. D. Chen, S. S. Xie, *Adv. Mater.* **2014**, *26*, DOI: 10.1002/adma.201400143.

[22] G. H. Yu, L. B. Hu, M. Vosgueritchian, H. L. Wang, X. Xie, J. R. McDonough, X. Cui, Y. Cui, Z. N. Bao, *Nano Lett.* **2011**, *11*, 2905.

[23] L. L. Zhang, X. Zhao, M. D. Stoller, Y. W. Zhu, H. X. Ji, S. Murali, Y. P. Wu, S. Perales, B. Clevenger, R. S. Ruoff, *Nano Lett.* **2012**, *12*, 1806.

[24] Y. Meng, Y. Zhao, C. Hu, H. Cheng, Y. Hu, Z. Zhang, G. Shi, L. Qu, *Adv. Mater.* **2013**, *25*, 2326.

[25] F. Meng, Y. Ding, *Adv. Mater.* **2011**, *23*, 4098.

[26] Z. Bo, W. Zhu, W. Ma, Z. Wen, X. Shuai, J. Chen, J. Yan, Z. Wang, K. Cen, X. Feng, *Adv. Mater.* **2013**, *25*, 5799.

[27] Z. Dong, C. Jiang, H. Cheng, Y. Zhao, G. Shi, L. Jiang, L. Qu, *Adv. Mater.* **2012**, *24*, 1856.

[28] L. F. Chen, Z. H. Huang, H. W. Liang, Q. F. Guan, S. H. Yu, *Adv. Mater.* **2013**, *25*, 4746.

[29] L. Liu, Z. Niu, L. Zhang, X. Chen, *Small* **2014**, *10*, DOI: 10.1002/smll.201400144.

[30] S. Y. Yin, Z. Q. Niu, X. D. Chen, *Small* **2012**, *8*, 2458.

[31] C. Choi, J. A. Lee, A. Y. Choi, Y. T. Kim, X. Lepró, M. D. Lima, R. H. Baughman, S. J. Kim, *Adv. Mater.* **2014**, *26*, 2059.

[32] Q. Meng, H. Wu, Y. Meng, K. Xie, Z. Wei, Z. Guo, *Adv. Mater.* **2014**, DOI: 10.1002/adma.201400399.

[33] Y. Xu, Z. Lin, X. Huang, Y. Wang, Y. Huang, X. Duan, *Adv. Mater.* **2013**, *25*, 5779.

[34] K. Jost, C. R. Perez, J. K. McDonough, V. Presser, M. Heon, G. Dion, Y. Gogotsi, *Energy Environ. Sci.* **2011**, *4*, 5060.

[35] L. B. Hu, M. Pasta, F. La Mantia, L. F. Cui, S. Jeong, H. D. Deshazer, J. W. Choi, S. M. Han, Y. Cui, *Nano Lett.* **2010**, *10*, 708.

[36] L. B. Hu, W. Chen, X. Xie, N. A. Liu, Y. Yang, H. Wu, Y. Yao, M. Pasta, H. N. Alshareef, Y. Cui, *ACS Nano* **2011**, *5*, 8904.

[37] H. Wang, B. W. Zhu, W. C. Jiang, Y. Yang, W. R. Leow, H. Wang, X. D. Chen, *Adv. Mater.* **2014**, *26*, doi:10.1002/adma.201305682.

[38] X. H. Lu, T. Zhai, X. H. Zhang, Y. Q. Shen, L. Y. Yuan, B. Hu, L. Gong, J. Chen, Y. H. Gao, J. Zhou, Y. X. Tong, Z. L. Wang, *Adv. Mater.* **2012**, *24*, 938.

[39] L. H. Bao, X. D. Li, *Adv. Mater.* **2012**, *24*, 3246.

[40] Z. Q. Niu, W. Y. Zhou, J. Chen, G. X. Feng, H. Li, Y. S. Hu, W. J. Ma, H. B. Dong, J. Z. Li, S. S. Xie, *Small* **2013**, *9*, 518.

[41] G. Y. Zheng, Y. Cui, E. Karabulut, L. Wagberg, H. L. Zhu, L. B. Hu, *MRS Bull.* **2013**, *38*, 320.

[42] A. C. Siegel, S. T. Phillips, M. D. Dickey, N. Lu, Z. Suo, G. M. Whitesides, *Adv. Funct. Mater.* **2010**, *20*, 28.

[43] A. D. Mazzeo, W. B. Kalb, L. Chan, M. G. Killian, J. F. Bloch, B. A. Mazzeo, G. M. Whitesides, *Adv. Mater.* **2012**, *24*, 2850.

[44] L. Y. Yuan, B. Yao, B. Hu, K. F. Huo, W. Chen, J. Zhou, *Energy Environ. Sci.* **2013**, *6*, 470.

[45] W. J. Hyun, O. O. Park, B. D. Chin, *Adv. Mater.* **2013**, *25*, 4729.

[46] Z. J. Shi, G. O. Phillips, G. Yang, *Nanoscale* **2013**, *5*, 3194.

[47] Y. R. Kang, Y. L. Li, F. Hou, Y. Y. Wen, D. Su, *Nanoscale* **2012**, *4*, 3248.

[48] G. Y. Zheng, L. B. Hu, H. Wu, X. Xie, Y. Cui, *Energy Environ. Sci.* **2011**, *4*, 3368.

[49] Z. Weng, Y. Su, D. W. Wang, F. Li, J. H. Du, H. M. Cheng, *Adv. Energy Mater.* **2011**, *1*, 917.

[50] K. Z. Gao, Z. Q. Shao, X. Wu, X. Wang, Y. H. Zhang, W. J. Wang, F. J. Wang, *Nanoscale* **2013**, *5*, 5307.

[51] N. D. Luong, N. Pahimanolis, U. Hippi, J. T. Korhonen, J. Ruokolainen, L. S. Johansson, J. D. Nam, J. Seppala, *J. Mater. Chem.* **2011**, *21*, 13991.

[52] K. Ariga, Y. Yamauchi, G. Rydzek, Q. M. Ji, Y. Yonamine, K. C. W. Wu, J. P. Hill, *Chem. Lett.* **2014**, *43*, 36.

[53] X. Xu, K. X. Sheng, C. Li, G. Q. Shi, *ACS Nano* **2010**, *4*, 4324.

[54] S. Y. Yin, Y. Y. Zhang, J. H. Kong, C. J. Zou, C. M. Li, X. H. Lu, J. Ma, F. Y. C. Boey, X. D. Chen, *ACS Nano* **2011**, *5*, 3831.

[55] X. Cao, D. Qi, S. Yin, J. Bu, F. Li, C. F. Goh, S. Zhang, X. Chen, *Adv. Mater.* **2013**, *25*, 2957.

[56] S. Yin, Y. Goldovsky, M. Herzberg, L. Liu, H. Sun, Y. Zhang, F. Meng, X. Cao, D. D. Sun, H. Chen, A. Kushmaro, X. Chen, *Adv. Funct. Mater.* **2013**, *23*, 2972.

[57] Q. M. Ji, I. Honma, S. M. Paek, M. Akada, J. P. Hill, A. Vinu, K. Ariga, *Angew. Chem. Int. Ed.* **2010**, *49*, 9737.

[58] Z. Q. Niu, L. Zhang, L. Liu, B. Zhu, H. Dong, X. Chen, *Adv. Mater.* **2013**, *25*, 4035.

[59] Z. Q. Niu, J. J. Du, X. B. Cao, Y. H. Sun, W. Y. Zhou, H. H. Hng, J. Ma, X. D. Chen, S. S. Xie, *Small* **2012**, *8*, 3201.

[60] Z. Q. Niu, J. Chen, H. H. Hng, J. Ma, X. D. Chen, *Adv. Mater.* **2012**, *24*, 4144.

[61] Y. Meng, K. Wang, Y. Zhang, Z. Wei, *Adv. Mater.* **2013**, *25*, 6985.

[62] K. Wang, Q. Meng, Y. Zhang, Z. Wei, M. Miao, *Adv. Mater.* **2013**, *25*, 1494.

[63] C. Long, D. Qi, T. Wei, J. Yan, L. Jiang, Z. Fan, *Adv. Funct. Mater.* **2014**, DOI: 10.1002/adfm.201304269.

[64] Z. Q. Niu, P. S. Lu, Q. Shao, H. B. Dong, J. Z. Li, J. Chen, D. Zhao, L. Cai, W. Y. Zhou, X. D. Chen, S. S. Xie, *Energy Environ. Sci.* **2012**, *5*, 8726.

[65] Q. Wu, Y. X. Xu, Z. Y. Yao, A. R. Liu, G. Q. Shi, *ACS Nano* **2010**, *4*, 1963.

[66] J. J. Xu, K. Wang, S. Z. Zu, B. H. Han, Z. X. Wei, *ACS Nano* **2010**, *4*, 5019.

[67] D. W. Wang, F. Li, J. P. Zhao, W. C. Ren, Z. G. Chen, J. Tan, Z. S. Wu, I. Gentle, G. Q. Lu, H. M. Cheng, *ACS Nano* **2009**, *3*, 1745.

[68] Z. S. Wu, A. Winter, L. Chen, Y. Sun, A. Turchanin, X. L. Feng, K. Mullen, *Adv. Mater.* **2012**, *24*, 5130.

[69] C. Z. Meng, C. H. Liu, L. Z. Chen, C. H. Hu, S. S. Fan, *Nano Lett.* **2010**, *10*, 4025.

[70] D. A. Dikin, S. Stankovich, E. J. Zimney, R. D. Piner, G. H. B. Dommett, G. Evmenenko, S. T. Nguyen, R. S. Ruoff, *Nature* **2007**, *448*, 457.